Original article

Screening and Identification of Herbal Urease Inhibitors Using Surface Plasmon Resonance Biosensor

Mahmood Biglar[1] , Hafezeh Salehabadi[2], Safoura Jabbari[3], Bahareh Dabirmanesh[3], Khosro Khajeh[3], Faraz Mojab[4], Massoud Amanlou[1,2*]

[1]Drug Design and Development Research Center, The Institute of Pharmaceutical Sciences (TIPS), Tehran University of Medical Sciences, Tehran, Iran.
[2]Department of Medicinal Chemistry, Faculty of Pharmacy, Tehran University of Medical Sciences, Tehran, Iran.
[3]Department of Biochemistry, Faculty of Biological Sciences, Tarbiat Modares University, Tehran, Iran.
[4]Department of Pharmacognosy, Faculty of Pharmacy, Shahid Beheshti University of Medical Sciences, Tehran, Iran.

Abstract

Background and objectives: Urease, that catalyzes the hydrolysis of urea, has received substantial attention for its impact on living organisms' health and human life quality. Urease inhibitors play important role in management of different diseases including gastritis and other gastrointestinal disorders. In the present study, a new surface plasmon resonance-based biosensor was designed to discover new urease inhibitors. **Methods:** The biosensor surface was prepared by the covalent immobilization of urease on carboxymethyldextran hydrogel (CMD 500D) via its primary amine groups. **Results:** The biosensor combined with an orthogonal enzyme inhibition assay was utilized for screening of 40 traditional medicinal plant extracts against Jack-bean urease. Among them, *Laurus nobilis* leaf extract displayed a high affinity with the immobilized urease; therefore, its active compound (quercetin) was isolated and identified as a urease inhibitor. The equilibrium constant (K_D) and Gibbs free energy ($\Delta G_{binding}$) values for the interaction of quercetin with urease were obtained to be 55 nM and -41.62 kJ/mol, respectively. The results of molecular docking analysis also confirmed our findings. **Conclusion:** This SPR-based biosensor represents a new, fast, reliable, and an accurate technique for the identification of new urease inhibitors or novel 'lead' compounds from natural resources.

Keywords: drug discovery; *Laurus nobilis;* surface plasmon resonance; urease inhibitors

Introduction

Helicobacter pylori is a Gram-negative bacterium which is able to adapt and survive in a highly acidic environment, such as the human stomach. *Helicobacter pylori* infection can instigate gastric inflammation and increase the risk of intestinal and gastric ulcers, gastric lymphoma, and gastric adenocarcinoma [1]. High-level expression of the urease enzyme in the *H. pylori* cytoplasm is the key virulence factor leading to such pathogens [2]. Urease (urea amidohydrolase; E.C. 3.5.1.5) is a nickel-containing enzyme that hydrolyzes urea to ammonia (NH_3) and carbon dioxide [3]. The formation of NH_3 brings about an increase in the medium pH, which provides a proper situation for *H. pylori* colonization and survival [4]. Therefore, it is possible to control the virulence

---

factors of *H. pylori* using the substances that can inhibit urease activity. Numerous urease inhibitors have been introduced in literature, such as hydroxamic acid derivatives, phosphorodiamidates, polyhalogenated benzo- and naphthoquinones, and imidazoles. These compounds have some weaknesses, including toxicity, chemical or physical instability, and low bioavailability, which limit their clinical use [5-8]. Discovering new urease inhibitors with a novel structure, greater stability, and lower toxicity is of critical importance and is essential to improve the life quality of human beings, animals, and plants. Undoubtedly, nature is a rich source of natural products, exhibiting a wide variety of biological activities. Natural products with a great diversity of chemical structures play a significant role in the pharma-botanical industry. Hence, investigating plant-derived natural products as urease inhibitors can offer excellent potential for treating diseases associated with severe urease activity and *H. pylori* infection [9-12].

Because of the chemical diversity of natural products, the investigation of Pan Assay Interference Compounds (PAINS) gains importance. PAINS cause false-positive assay readouts due to the multiple behaviors under assay conditions, such as metal chelation, fluorescence effects, cysteine oxidation, and redox cycling [13,14]. An orthogonal screening approach, in which a biophysical assay is combined with a biochemical assay, would help to identify PAINS [15-17]. Hence, the surface plasmon resonance (SPR) technique was used as a biophysical assay [18,19]. SPR is an optical detection technique which makes it possible to observe the binding of an analyte to a surface-immobilized target molecule. SPR has attracted much attention as a biosensor, because it is a direct, label free and real time procedure; therefore, it is useful for affinity analysis [20-22]. This paper aimed to use the SPR technology, as an orthogonal screening approach, for the discovery and examination of urease inhibitors. Thus, a carboxymethyldextran hydrogel sensor chip (CMD 500D) was utilized to immobilize urease using amine coupling reagents. The molecular docking was used to confirm the results of the SPR technique [23].

Material and Methods

Ethical considerations

Ethical approval for this study was granted by the Ethical Committee of The Institute of Pharmaceutical Sciences, Tehran University of Medical Sciences, Tehran, Iran (Reference number: TIPS-902-46-95-12-24).

Chemicals

Jack-bean urease (EC 3.5.1.5) was purchased from Sigma (St. Louis, MO, USA). Dimethyl sulfoxide, methanol (HPLC grade), ethyl acetate, chloroform, silica gel (70–30 mesh) and thin-layer chromatography (TLC) plates (silica gel 60F 254+366) were obtained from Merck Co. (Germany). Deionized water was used in all the experiments.

The carboxymethyl dextran (CMD 500D) sensor chip and the amine-coupling kit containing N-hydroxysuccinimide (NHS), N-Ethyl-N′-(3-dimethylaminopropyl) carbodiimide, and ethanolamine hydrochloride were obtained from Xantec Bioanalytics (Germany).

Plant material

The herbal materials were obtained from local medicinal herb shops, Tehran, Iran (June 2016). These plants were identified by one of the authors of this study (Prof. F. Mojab). The authenticated samples were deposited at the Herbarium of School of Pharmacy, Shahid Beheshti University of Medical Sciences (Supplementary Table 1).

Instruments

Infrared (IR) spectra were recorded on a PerkinElmer Model 781 spectrometer using IR grade potassium bromide (KBr) disks. ^{1}H NMR spectra of synthesized compounds were recorded on a Varian Inova 500 spectrometer (Bruker, Darmstadt, Germany). Tetramethylsilane (TMS) and DMSO-d_6 were used as the internal standard and solvent, respectively.

Preparation of extracts from plants

One g of air-dried and powdered plant material of each of the forty species was extracted using 10 mL of 80:20 methanol/water at room temperature (25 ± 1 ℃) for 24 h, followed by 2-hour sonication in an ultrasonic bath. The resulting liquid extract was then filtered and concentrated to dryness under reduced pressure and freeze dried. The dry extracts were stored at -20 ℃ to be used later [24].

Isolation of quercetin from *Laurus nobilis*

The powdered leaves of *L. nobilis* (100 g) were

subjected to extraction with 2000 mL of methanol/water (80:20, v/v) at room temperature (25 ± 1 °C) for 24 hours, followed by 2-hour sonication in an ultrasonic bath. The extract was then concentrated using a rotary evaporator and stored at 4 °C. The hydroalcoholic extract was then concentrated and extracted successively with hexane and ethyl acetate. Repeated chromatography of the active ethyl acetate extract on silica gel and Sephadex LH-20 (Mitsubishi Kasei Co., Ltd) columns resulted in the isolation of quercetin [25].

Preparation of stock solutions

Herbal extract solutions from different plants were prepared via dissolving 1 mg of the dried extracts in 1 mL of the phosphate buffer solution (10 mM, pH 7.5) and diluting them at a final concentration of 330 µg/mL [26,27]. The standard quercetin solution was prepared by dissolving 0.302 mg of quercetin in 1 mL (1 mM) of the phosphate buffer solution (10 mM, pH 8.5). Working solutions in the range of 1 pM - 1 mM of quercetin were prepared by appropriate dilution of the stock solutions in phosphate buffer. Urease solution was prepared by suspending 3 mg of enzyme with 1 mL of 100 mM phosphate buffer, pH 7.5. The suspension was gently swirled at room temperature for 2 min. Subsequently, the mixture was centrifuged at 4000 g for 5 min at 4 °C. The supernatant was used for further analysis of the urease activity assay. The Bradford protocol was used to determine the protein concentration in the supernatant.

Urease inhibition assay

The urease inhibition activity was determined through the modified spectrophotometric method based on the Berthelot reaction. Hydroxyurea was employed as a standard inhibitor (IC_{50}=7.6 µg/mL). The solution assay mixture consisted of 850 µL of urea (30 mM) and 135 µL of the inhibitor (330 µg/mL) with a total volume of 985 µL. The enzymatic reactions initiated via the addition of 15 µL of the urease enzyme solution (1 µg/mL) in phosphate buffer (100 mM, pH 7.4). After 30 min, the urease activity was determined by measuring the ammonia concentration. The ammonia concentration was determined using 500 µL of Solution A (containing 0.5 g of phenol and 2.5 mg of sodium nitroprusside in 50 mL of distilled water) and 500 µL of Solution B (containing 250 mg of sodium hydroxide and 820 µL of sodium hypochlorite 5% in 50 mL of distilled water) at 37 °C for 30 min. The absorbance was detected at 625 nm. The activity of the uninhibited urease was designated as the control activity of 100% [28].

Data processing and determination of IC_{50} value for quercetin

The extent of the enzymatic reaction was calculated based on the following equation:

$$I\,(\%) = 100 - 100 \times (T\,/\,C)$$

Where I (%) is enzyme inhibition, T (test) is the absorbance value for the tested sample (quercetin, plant extracts, or the positive control in the solvent) in the presence of the enzyme, and C (control) is the absorbance value of the solvent in the presence of the enzyme. The IC_{50} value (the concentrations of test compounds that inhibit the hydrolysis of substrates by 50 %) was determined by measuring the quercetin urease inhibitory activity at various quercetin concentrations. The IC_{50} value was obtained from dose-response curves using GraphPad Prism software (Version 5).

Immobilization of urease onto CMD chip surface

The enzyme was immobilized via its primary amine groups through EDC/NHS esters [29,30]. In order to immobilize urease, 250 µL of urease solution (87 µg in 10 mM acetate buffer, pH 4.5) was injected over the activated chip. The remaining active sites of the SPR sensor were blocked by 1 M ethanolamine (pH 8.5). The amount of immobilized enzyme was determined by subtracting the concentration of urease before and after passing over the chip surface. Urease solution (250 µL) with concentration of 87 µg was injected over the activated chip. The solution was then collected after passing through the chip and its concentration was determined to be 40 µg by Bradford method. Therefore, the absolute amount of enzyme immobilized on the chip surface was about 47 µg. The SPR SR7500DC instrument (XanTec bioanalytics GmbH, Germany) detects changes in the refractive index and measures these changes in microrefractive-index units (µRIU). A change in the refractive

index is commensurate with the quantity (mass) of the analyte interacting with the surface.

SPR measurements

To study the interaction between the analyte (the plant extracts and/or quercetin) and the immobilized urease, the analyte flowed over the sensor surface. After optimizing the pH condition, 0.1 nM to 1 mM of quercetin or 33 µg/mL of the plant extracts in 10 mM phosphate buffer (pH 7.5) were individually injected over the urease immobilized CMD surface and the reference protein, human serum albumin (HSA), for 5 min with a flow rate of 50 µL/min at 25 °C. A blank control run was undertaken by injecting the above-mentioned buffers, and the bulk effects were corrected by solvent corrections. Reference sensorgrams were subtracted from binding sensorgrams using the Scrubber analysis program (Biologic Software Pty. Ltd., Canberra, Australia).

## Atomic force microscopy (AFM)

The surface topology images of the CMD SPR chip before and after urease immobilization were obtained via an AFM apparatus (Veeco-Autoprobe-CP-research, Santa Barbara, CA). The AFM imaging was achieved in non-contact mode in air at room temperature. A resolution of 256 pixels was utilized for all the AFM images.

Docking studies

The optimized structure of the protein and ligand was used as the input for the consequent docking studies. The AutoDockTools program (ADT; version 1.5.6) was utilized to prepare the protein and ligand [31]. Jack bean urease at X-ray diffraction 2.05 Å resolution (PDB ID: 3LA4) was derived from the RCSB Protein Data Bank (www.rcsb.org). Water molecules were omitted, polar hydrogens were added to the protein structure, and Kollman charges were assigned to all atoms of the enzyme. The chemical structure of the ligand was generated by HyperChem software (Version 8.0), hydrogens were added, and energy minimization was performed by molecular mechanics and semi-empirical molecular orbital methods. Grid maps were generated by AutoGrid 4.2 software [31]. All maps were calculated with 0.375 Å spacing between grid points. Each docked system was carried out by 100 runs using AutoDock 4.2 [31].

Results and Discussion

The detection and elimination of PAINS in drug discovery assays, especially in high throughput screening (HTS), has attracted enormous attention recently [16]. Hence, the main focus of the present study was to develop an SPR-based assay for investigating the interaction between urease and its inhibitors. The analysis of the urease structure revealed that about 80% of lysine and arginine residues were located at the protein surface, far enough away from the active site (Figure 1). The orientation of the distribution of the mentioned residues reduced the random coupling of urease and increased the sensitivity of the sensor. Therefore, it was decided to immobilize the enzyme via amine groups.
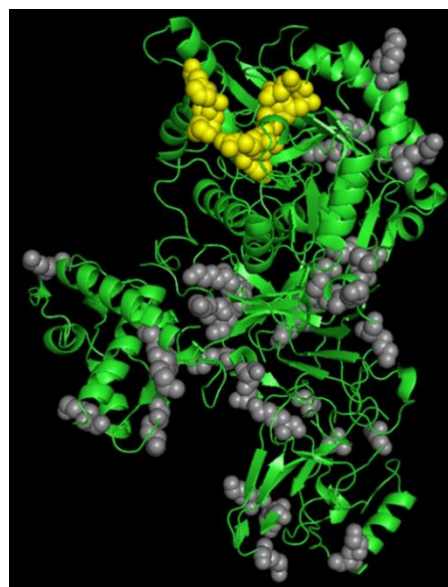

Figure 1. Side view of the three-dimensional model of urease from jack bean (PDB code: 3LA4) as the template. The model shows that lysine and arginine residues (gray sphere) are located far away from the active site (yellow sphere).

Based on our analysis, Jack-bean urease was successfully immobilized on the CMD 500D sensor chip by amine coupling using EDC/NHS (Figure 2). The signal up to 2500 µRIU was achieved through enzyme immobilization. Therefore, it was ensured that the analyte with low molecular weight could produce a measurable change in refractive index [29,30]. The atomic force microscopy (AFM) images of immobilized and bare CMD surface in both two and three-dimensional views are shown in Figure 3. Urease was homogeneously distributed over the CMD chip. Furthermore, the average surface roughness increased from 0.217 nm to 0.405 nm.
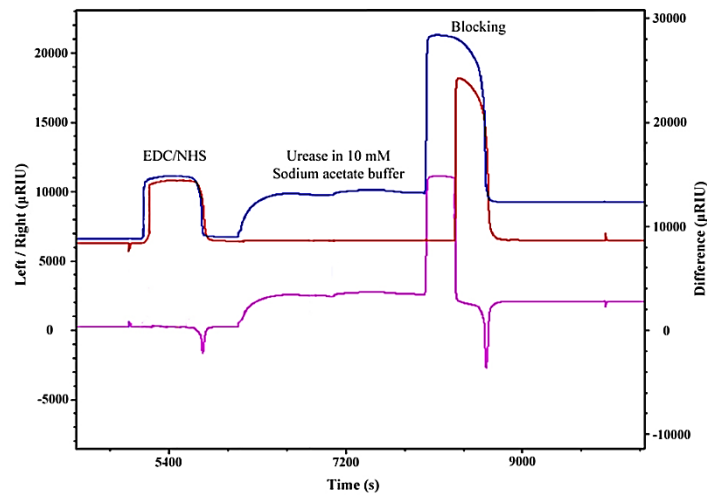
Figure 2. Sensogram for covalent immobilization of urease onto SPR-CMD surface; carrier solution: 10 mM phosphate buffer (pH 7.5), flow speed 25 µL/min; The pink line indicates the difference between blue (immobilized ligand channel) and red (reference channel) line. After EDC/NHS activation of both channels, urease was just injected over one channel (blue line), and then both surfaces were blocked ethanolamine. The increasing signal up to 2500 µRIU (pink line) demonstrates the proper immobilization of urease.
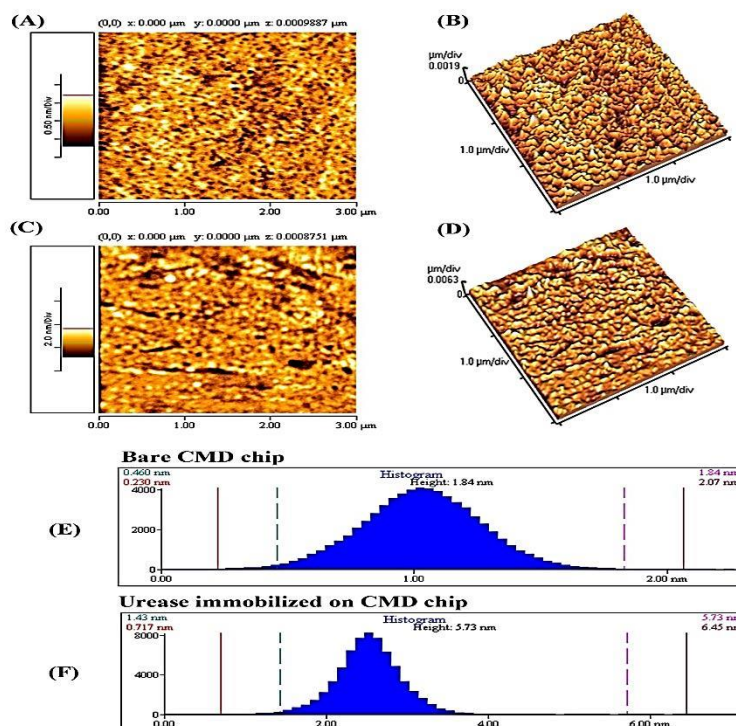
Figure 3. Two and three-dimensional AFM micrographs of bare (A, B) and immobilized surface (C, D). Height distribution diagrams are shown at the bottom (E and F). The AFM images along with the height distribution diagrams indicate a larger height difference on the urease immobilized surface (right) than the bare CMD surface (left).

Undoubtedly, due to their active chemical constituents, medicinal plants are considered as significant resources to develop new drugs [11]. In the current study, the urease inhibitory activity of forty medicinal plant extracts (traditionally employed to treat stomach and gastric diseases) was investigated based on the Berthelot reaction. As seen in Table 1, six extracts exhibited more than 80% inhibitory activity at a concentration of 330 μg/mL. The potent extracts were selected to determine the IC_{50} values and they were further tested via enzyme-based SPR biosensors. The IC_{50} values of these extracts are shown in Table 2. The selected herbal extracts with a concentration of 33 μg/mL were injected over the immobilized enzyme. To monitor the ligand-binding tendency and activity of the immobilized enzyme, urea, as

a known urease substrate was injected over immobilized urease. Analysis of the collected product by Berthelot reaction demonstrated the catalytic activity of the immobilized enzyme and confirmed the active site accessibility after immobilization. Also, the consecutive injections of hydroxyurea, as a positive control, confirmed the stability of the surface and the activity of urease in each experiment. As shown in Figure 4, the corresponding SPR signal increased with the injection of plant extracts onto the CMD chip. When the ligand-enzyme binding process reached equilibrium, the running buffer was passed over the sensor, the analyte was dissociated from urease and the SPR signal decreased. Eventually, the SPR signals returned to the baseline.

Table 1. Urease inhibition activity of the 40 studied plants

No	Scientific name and plant family	Common name	Part used	Inhibition (%)
1	*Acorus calamus* L. (Acoraceae)	Sweet flag	Root	69.46 ± 0.65^a
2	*Achillea millefolium* L. (Asteraceae)	Yarrow	Flower	48.89 ± 1.32
3	*Allium cepa* L. (Amaryllidaceae)	Onion	Seed	34.42 ± 0.51
4	*Allium sativum* L. (Amaryllidaceae)	Garlic	Rhizome	39.63 ± 0.18
5	*Allium schoenoprasum* L. (Amaryllidaceae)	Chives	Leaf	46.01 ± 0.32
6	*Angelica archangelica* (Apiaceae)	Garden angelic	Root	65.45 ± 0.43
7	*Asclepias syriaca* L. (Apocynaceae)	Milkweeds	Seed	28.02 ± 0.87
8	*Brassica nigra* L. (Brassicaceae)	Black Mustard	Seed	9.00 ± 0.61
9	*Berberis integerrima* Bunge. (Berberidaceae)	Berberis	Fruit	43.08 ± 0.86
10	*Boswellia carterii* Birdw.(Burseraceae)	Frankincense	Resin	13.43 ± 1.20
11	*Cerasus avium* (L.) Moench. (Rosaceae)	Sweet cherry	Tail	17.64 ± 0.28
12	*Citrullus colocynthis* (L.) Schrad. (Cucurbitaceae)	Bitter apple	Fruit	59.08 ± 1.02
13	*Citrus aurantifolia* (Christm.) (Rutaceae)	Key lime	Fruit	34.59 ± 1.27
14	*Citrus aurantium* L. (Rutaceae)	Bitter orange	Flower	34.52 ± 0.63
15	*Colchicum* sp. (Colchicaceae)	Crocus	Rhizome	43.81 ± 0.72
16	*Crocus sativus* L. (Iridaceae)	Saffron	Stigma	10.67 ± 0.81
17	*Datura stramonium* L. (Solanaceae)	jimsonweed	Leaf	8.98 ± 1.26
18	*Dorema ammoniacum* Don. (Umbelliferae)	Gum ammoniac	Resin	11.19 ± 0.4
19	*Fraxinus velutina* L. (Velvet Ash)	Zaban-e ghonjeshk	Leaf	18.46 ± 0.31
20	*Foeniculum vulgar* L. (Apiaceae)	Fennel seed	Seed	29.73 ± 0.67
21	*Humulus lupulus* L. (Cannabinaceae)	Hops	Twig	31.58 ± 1.1
22	*Heracleum persicum* Desf. (Apiaceae)	Persian hogweed	Seed	58.87 ± 0.25
23	*Helianthus tuberosus* L. (Asteraceae)	Earth apple	Root	19.22 ± 0.62
24	*Hyssopus officinalis* L. (Labiatae)	Hyssos	Herb	9.25 ± 0.33
25	*Laurus nobilis* L. (Lauraceae)	Grecian laurel	Leaf	89.26 ± 0.12
26	*Malva sylvestris* L. (Malvaceae)	Creeping charlie	Flower	15.71 ± 0.2
27	*Matricaria recutita* L. (Asteraceae)	Chamomile	Flower	83.66 ± 0.63
28	*Morus alba* L. (Moraceae)	White mulberry	Leaf	5.13 ± 1.09
29	*Nardostachys jatamansi* L. (Caprifoliaceae)	Spikenard	Rhizomes	3.45 ± 0.57
30	*Nigella sativa* L. (Ranunculaceae)	Black Cumin	Seed	75.18 ± 0.67
31	*Onopordum acanthium* L. (Asteraceae)	Cotton thistle	Seed	36.98 ± 0.11
32	*Peganum harmala* L. (Nitrariaceae)	Wild rue	Seed	51.73 ± 0.57
33	*Piper nigrum* L. (Piperaceae)	Black pepper	Seed	25.36 ± 0.35
34	*Quercus alba* L. (Fagaceae)	White oak	Leaf	29.65 ± 1.12
35	*Rubia tinctorum* L. (Rubiaceae)	Madder	Root	30.72 ± 0.67
36	*Rubus* sp. L. (Rosaceae)	Blackberry	Leaf	15.43 ± 0.31
37	*Spinacia oleracea* L. (Amaranthaceae)	Spinach	Leaf	9.29 ± 0.18
38	*Trigonella foenum-graecum* L. (Fabaceae)	Fenugreek	Leaf	26.31 ± 0.83
39	*Teucrium polium* L. *(*Lamiaceae)	Felty germander	Aerial part	61.73 ± 0.16
40	*Zingiber officinale* L. (Zingiberaceae)	Ginger	Rhizome- root	79.8 ± 0.42

[a]Values are expressed as mean ± SD of 3 experiments

Table 2. The IC$_{50}$ (µg/mL) and the percent of urease enzyme inhibition of the most active medicinal plants

| Scientific name	Plant family	Part used	Inhibition (%)	IC$_{50}$ (µg/mL)
Acours calamus	Araceae	Root	69.46	68.35
Angelica archangelica	Apiaceae	Leaf	65.45	74.97
Laurus nobilis	Lauraceae	Leaf	89.26	36.28
Matricaria chamomilla	Chamomile	Flower	83.66	42.76
Nigella sativa	Ranun Culaceae	Seed	75.18	55.17
Zingiber officinale	Zingiberaceae	Rhizome- root	79.80	46.53
Quercetin	-	-	-	9.47
Hydroxyurea	-	-	-	7.60
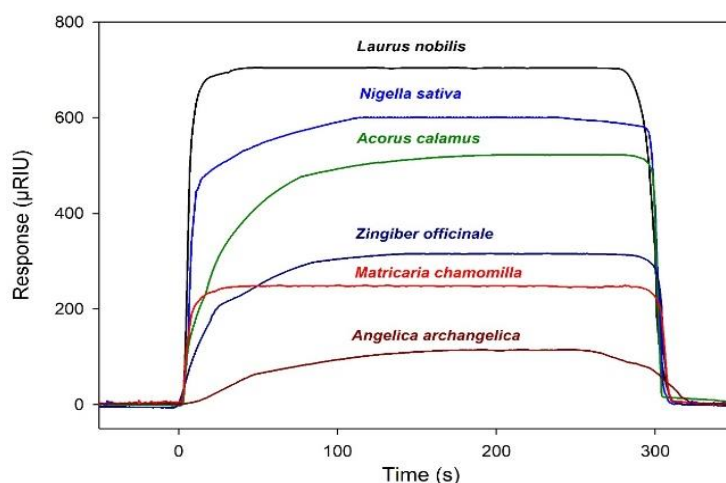
Figure 4. SPR response of interaction between herbal extracts and the immobilized urease; Six herbal extracts have been injected over the immobilized and reference chip surface. Reference sensorgram of each six extracts individually was subtracted from their binding sensorgram using the Scrubber analysis program, and six curves were compared with each other.

Among the chosen herbal extracts (*Acorus calamus, Angelica archangelica, Laurus nobilis, Matricaria chamomilla, Nigella sativa, and Zingiber officinale*), *Laurus nobilis* demonstrated the fastest association constant (k$_a$) and had a strong interaction with urease without requiring any regeneration solution (reversible binding); therefore, it was selected for future analysis. The achieved results were in line with the values obtained from the traditional Berthelot assay (see Table 2). High inhibition activity of *M. chamomilla* and *Z. officinale* was observed in Berthelot assay that might be attributed to the presence of tannins in these herbs [32,33]. It is clear that the phenolic compounds, such as tannins, can affect enzymatic activity.

Quercetin (Figure 5A) was isolated from *L. nobilis* extract as a yellow crystal. The yield of extraction was 15%. A detailed description of the method is provided in the previous study [25]. This compound was identified by melting point: mp 316-319 °C; FT-IR: IR (KBr) vmax cm^{-1} 3296, 1669, 1605, 1518, 1314, 1162, 1096 and ^{1}HNMR: 500 MHz, DMSO-*d6*; δ (ppm) 12.47 (1H, s, OH), 10.75 (1H, s, OH), 9.56 (1H, s, OH), 9.33 (1H, s, OH), 9.28 (1H, s, OH) 7.67 (1H, d, J = 2.4 Hz, H-2′), 7.53 (1H, dd, J = 8.5, 2.3 Hz, H-6'), 6.88 (1H, d, J = 8.5 Hz, H-5'), 6.40 (1H, d, J = 2.2 Hz, H-8), 6.18 (1H, d, J = 2.2 Hz, H-6).

After the covalent immobilization of the enzyme onto CMD 500D (via EDC/NHS), quercetin was injected simultaneously over both the immobilized urease and the reference channel. The variations of the SPR signal for different quercetin concentrations are depicted in Figure 5B. After the injection of quercetin, a fast and continuous response was observed, followed by a plateau, regeneration, and eventually a return to the initial baseline. Detecting small molecules (molecular weight <500 Da) is a big challenge in SPR assays [30]. In this biosensor, a suitable signal was obtained by immobilizing urease on CMD 500D as a 3D chip. 3D chips allow multilayer enzyme immobilization, which leads to significant signal amplification. The proper signal intensity of the interaction between urease and quercetin (MW= 302.2 Da) observed here clearly indicated that the SPR biosensor was capable of detecting the binding of low molecular weight analytes.
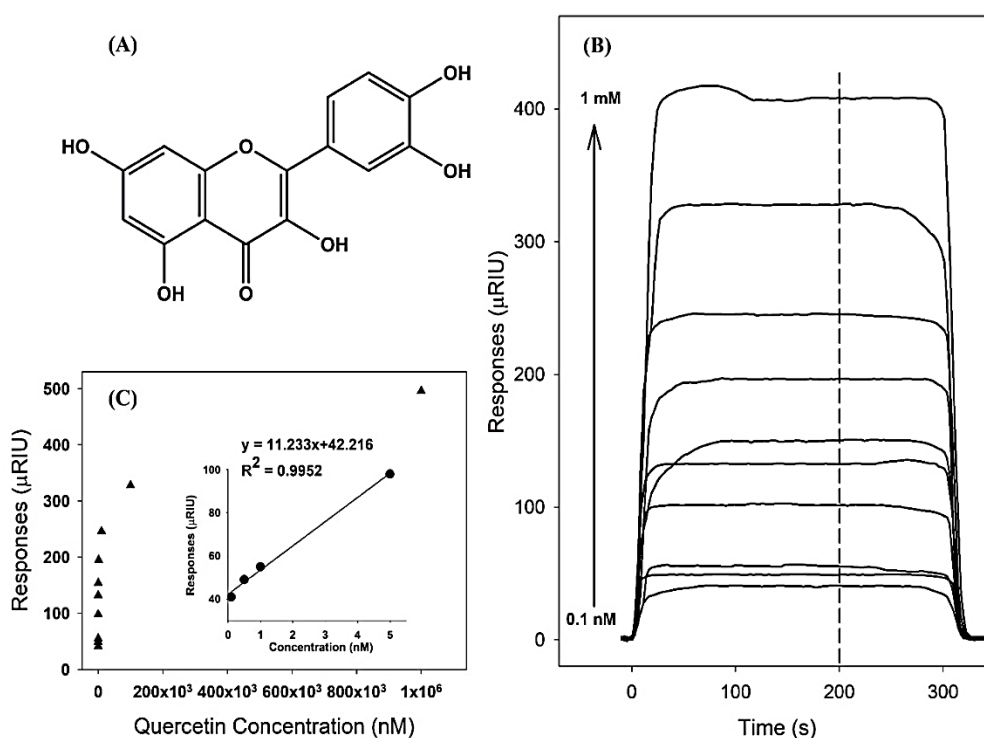
Figure 5. (A) Structure of quercetin isolated from *Laurus nobilis*; (B) SPR sensorgrams for the interaction of urease and quercetin; carrier solution: phosphate buffer, flow speed: 50 μL/min, flow duration: 5 mins, (C) Calibration curve in the linear detection range from 0.1 to 5 nM

Table 3. Kinetic parameters for the binding of quercetin with the immobilized urease

Parameter	k_a ($M^{-1}s^{-1}$)	k_d (s^{-1})	k_D (nM)	R_{max}	ΔG_b (kJ/mol)	Fitting model
Value	1.8×10^4	1×10^{-3}	55	962	-41.61	1:1

As shown in Figure 5C, the biosensor successfully illustrated a linear detection range from 0.1 to 5 nM. The LOD (limit of detection) and LOQ (limit of quantification) based on 3×(standard deviation of the blank/slope) and 10×(standard deviation of the blank/slope) turned out to be 35 and 120 pM, respectively. The SPR signals of the quercetin/urease interaction (Figure 5B) were used to calculate the equilibrium constant (K_D). To determine the association (k_a) and dissociation (k_d) constants, the kinetic Langmuir binding model 1:1 was fitted the interaction curves. The K_D value was utilized to calculate the thermodynamic parameters, using Van't Hoff equations [34]:

$$\Delta G_{binding} = -RT \ln K_A$$
$$K_A = 1/K_D$$

Where R is the ideal gas constant, K_A is the affinity constant, T is temperature, and $\Delta G_{binding}$

is changes in Gibb's free energy of the binding of quercetin with the immobilized urease. Table 3 presents the kinetic parameters for the binding of quercetin with the immobilized urease.

The relatively low value of K_D (55 nM) indicated a high affinity between the immobilized urease and quercetin [35]. The value of $\Delta G_{binding}$ turned out to be -41.61 kJ/mol (-9.94 kcal/mol). The negative value of $\Delta G_{binding}$ was in line with the results of the docking study presented in the next section, indicating the spontaneous interaction of quercetin with the immobilized urease on the CMD SPR chip.

The IC_{50} value for quercetin was also determined to be 31.36 μM (~ 9.47 μg/mL) using the Berthelot assay (see Figure S1; supplementary material). The K_D calculated by the SPR technique and the IC_{50} value determined by the enzymatic inhibition assay confirmed the inhibitory activity of quercetin against urease.
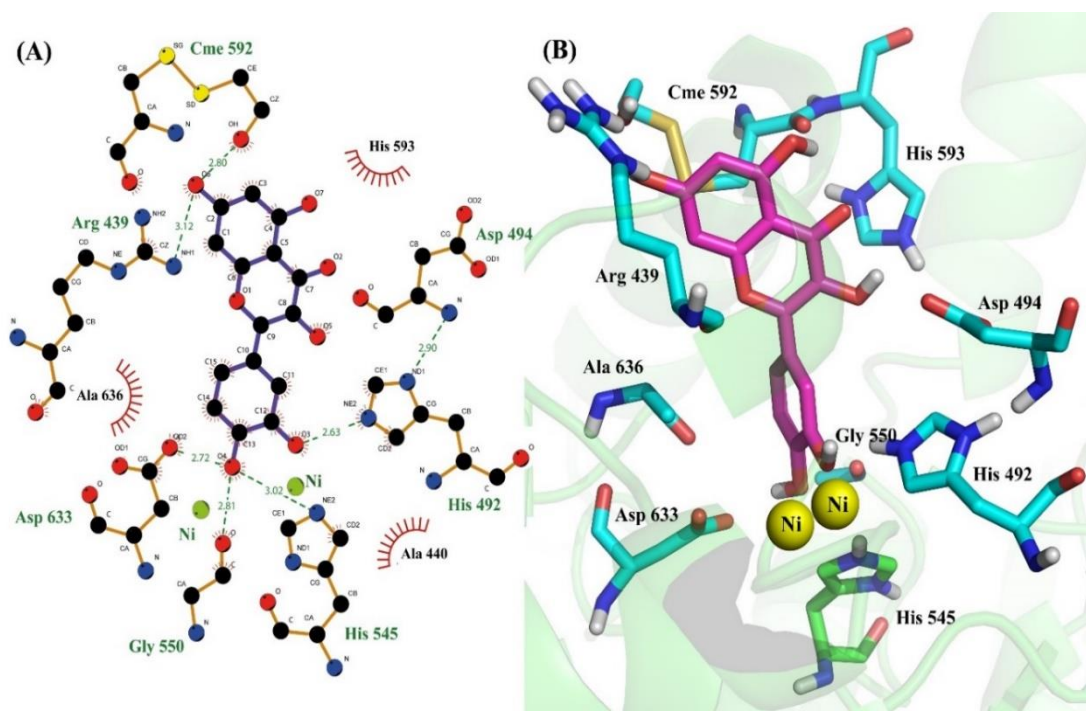
Figure 6. Interaction of the quercetin and urease; (A) two-dimensional representation; olive green arrow: H bond interaction, brick red representation; hydrophobic site. Nitrogen is blue, oxygen is red, carbon is black, nickel is green and sulfur is yellow. (B) Three-dimensional representation; the ligand is presented in magenta, the residues in blue and nickel ions are yellow spheres. The protein-ligand interaction was generated by the LigPlot[+] and PyMOL softwares.

The results presented here revealed that the SPR biosensor could be successfully employed for detection and evaluation of urease inhibitors.

The molecular docking was used to predict the orientation of quercetin in the urease binding pocket. The planar structure of quercetin made it possible to enter the active site cleft. In addition, the suitable positions of functional groups resulted in their appropriate interactions with the active site of the enzyme.

The docking results showed that the hydroxyl groups of the catechol ring inclined to interact with two nickel atoms in the center of the enzyme while the aromatic rings of quercetin had interactions with Ala440, His593, and Ala636 residues, which formed a hydrophobic cavity in the opening of the active site pocket. Also, hydrogen bonding was generated between the hydroxyl group in the 3,5,7- trihydroxy-4H-chromen-4-one ring and Arg439 and CME592. The hydroxyl group at the fourth position of the catechol ring played a considerable role in forming a hydrogen bond with His545, Gly550, and Asp633 (Figure 6). Thus, quercetin forms five hydrogen bonds with the urease enzyme. Moreover, water-mediated hydrogen bonds contributed to this tight binding; however, identifying these bindings through docking studies is quite difficult unless the crystal structure of this binding is achieved. The estimated binding free energy and inhibition constant (K_i) showed that quercetin was accurately docked into the active site of urease. The results indicated that the contributions of the van der Waals interactions are superior to the electrostatic interactions (Table S1; supplementary material).

Helicobacter pylori infection can encourage gastrointestinal diseases, especially gastritis, peptic ulcer, and gastric cancer. Its inhabitant in the acidic medium of the stomach is highly dependent on urease activity. Therefore, developing urease inhibitors is of critical importance. Moreover, due to offering excellent potential for drug discovery, medicinal plants have attracted numerous attentions and endeavors to find new natural products to treat gastritis diseases. To this end, various instrumental methods have been employed to analyze the urease inhibitor activity of various synthetic or natural compounds by measuring the release of ammonia during enzymatic reactions [26,27,36,37]. However, these approaches present a number of disadvantages, such as a lack of sensitivity, high urease consumption, and the involvement of organic solvents, which limit their applications. In the present study, an enzyme-based SPR biosensor method was

developed to improve the existing methods due to its label-free procedure, high sensitivity, and very simple and fast real-time analysis. The new enzyme-based SPR technique was utilized to investigate the interaction of the immobilized urease on the CMD chip with quercetin and the selected plant extracts as urease inhibitors. The SPR analysis (as binding assay) displayed a K_D value of 55 nM for quercetin, which is in agreement with the IC_{50} value (31.36 µM) obtained by enzymatic assay. These experimental results demonstrated a great affinity of quercetin from *L. nobolis* leaves with the immobilized urease. To consider the inhibitory function of quercetin more precisely, a protein-ligand docking simulation and a competitive inhibition experiment were carried out. The results were consistent with those of the SPR, confirming the binding of quercetin to the urease active site.

Conclusion

The most remarkable finding of this study was that quercetin was responsible for the urease inhibitory activity, and *L. nobolis* leaves extract could be used as a potent urease inhibitor for managing gastritis. In addition, the SPR-based biosensor could be an approach to improve drug discovery processes for many important classes of drug targets due to its great sensitivity.

Acknowledgments

Author contributions

Mahmood Biglar, Hafezeh Salehabadi, Safoura Jabbari and Bahareh Dabirmanesh contributed in the phytochemical and SPR experiments and wrote the first draft of the paper. Faraz Mojab contributed in the phytochemical experiment and identification of samples. Khosro Khajeh and Massoud Amanlou contributed in designing the experiments and final approval of the manuscript.

Declaration of interest

The authors declare that there is no conflict of interest. The authors alone are responsible for the accuracy and integrity of the paper content.

References

[1] Algood HMS, Cover TL. *Helicobacter pylori* persistence: an overview of interactions between *H. pylori* and host immune defenses. *Clin Microbiol Rev*. 2006; 19(4): 597–613.

[2] Sachs G, Scott DR, Wen Y. Gastric infection by *Helicobacter pylori*. *Curr Gastroenterol Rep*. 2011; 13(6): 540–546.

[3] Maroney MJ, Ciurli S. Nonredox nickel enzymes. *Chem Rev*. 2014; 114(8): 4206–4228.

[4] Stingl K, Altendorf K, Bakker EP. Acid survival of *Helicobacter pylori*: how does urease activity trigger cytoplasmic pH homeostasis? *Trends Microbiol*. 2002; 10(2): 70–74.

[5] Pedrazzini F, Tarsitano R, Nannipieri P. The effect of phenyl phosphorodiamidate on urease activity and ammonia volatilization in flooded rice. *Biol Fertility Soils*. 1987; 3(3): 183–188.

[6] Ashiralieva A, Kleiner D. Polyhalogenated benzo- and naphthoquinones are potent inhibitors of plant and bacterial ureases. *FEBS Lett*. 2003; 555(2): 367–370.

[7] Ndemangou B, Tedjon Sielinou V, Vardamides JC, Shaiq Ali M, Lateef M, Iqbal L, Afza N, Nkengfack AE. Urease inhibitory isoflavonoids from different parts of *Calopogonium mucunoides* (Fabaceae). *J Enzyme Inhib Med Chem*. 2013; 28(6): 1156–1161.

[8] Abid OUR, Babar TM, Ali FI, Ahmed S, Wadood A, Rama NH, Uddin R, Zaheer-Ul-Haq A, Khan A, Choudhary MI. Identification of novel urease inhibitors by high-throughput virtual and in vitro screening. *ACS Med Chem Lett*. 2010; 1(4): 145–149.

[9] Angelo de F, Luzia VM, Andreia CCS, Raphael RP. Wound healing agents: the role of natural and non-natural products in drug development. *Mini-Rev Med Chem*. 2008; 8(9): 879–888.

[10] Dayan FE, Cantrell CL, Duke SO. Natural products in crop protection. *Biorg Med Chem*. 2009; 17(12): 4022–4034.

[11] Cragg GM, Newman DJ. Natural products: a continuing source of novel drug leads. *Biochim Biophys Acta Gen Subj*. 2013; 1830(6): 3670–3695.

[12] De Fatima A, Terra BS, Da Silva CM, Da Silva DL, Araujo DP, Da Silva Neto L, Nascimento de Aquino RA. From nature to market: examples of natural products that became drugs. *Recent Pat Biotechnol*. 2014;

8(1): 76–88.

[13] Baell JB. Feeling nature's pains: natural products, natural product drugs, and pan assay interference compounds (PAINS). *J Nat Prod*. 2016; 79(3): 616–628.

[14] Pouliot M, Jeanmart S. Pan assay interference compounds (PAINS) and other promiscuous compounds in antifungal research. *J Med Chem*. 2016; 59(2): 497–503.

[15] Aldrich C, Bertozzi C, Georg GI, Kiessling L, Lindsley C, Liotta D, Merz KM, Schepartz A, Wang S. The ecstasy and agony of assay interference compounds. *ACS Cent Sci*. 2017; 3(3): 143–147.

[16] Christopeit T, Carlsen TJO, Helland R, Leiros HKS. Discovery of novel inhibitor scaffolds against the metallo-β-lactamase vim-2 by surface plasmon resonance (spr) based fragment screening. *J Med Chem*. 2015; 58(21): 8671–8682.

[17] Jasial S, Hu Y, Bajorath J. How frequently are pan-assay interference compounds active? Large-scale analysis of screening data reveals diverse activity profiles, low global hit frequency, and many consistently inactive compounds. *J Med Chem*. 2017; 60(9): 3879–3886.

[18] Redhead M, Satchell R, Morkūnaitė V, Swift D, Petrauskas V, Golding E, Onions S, Matulis D, Unitt JA. A combinatorial biophysical approach; FTSA and SPR for identifying small molecule ligands and PAINs. *Anal Biochem*. 2015; 479: 63–73.

[19] Davis BJ, Erlanson DA. Learning from our mistakes: the 'unknown knowns' in fragment screening. *Bioorg Med Chem Lett*. 2013; 23(10): 2844–2852.

[20] Patching SG. Surface plasmon resonance spectroscopy for characterisation of membrane protein-ligand interactions and its potential for drug discovery. *Biochim Biophys Acta*. 2014; 1838(1, Pt A): 43–55.

[21] Xiang Y, Kiseleva R, Reukov V, Mulligan J, Atkinson C, Schlosser R, Vertegel A. Relationship between targeting efficacy of liposomes and the dosage of targeting antibody using surface plasmon resonance. *Langmuir*. 2015; 31(44): 12177–12186.

[22] Ding X, Yang KL. Development of an oligopeptide functionalized surface plasmon resonance biosensor for online detection of glyphosate. *Anal Chem*. 2013; 85(12): 5727–5733.

[23] Modolo LV, de Souza AX, Horta LP, Araujo DP, de Fátima Â. An overview on the potential of natural products as ureases inhibitors: a review. *J Adv Res*. 2015; 6(1): 35–44.

[24] Sharifi N, Souri E, Ziai SA, Amin G, Amanlou M. Discovery of new angiotensin converting enzyme (ACE) inhibitors from medicinal plants to treat hypertension using an in vitro assay. *DARU J Pharm Sci*. 2013; 21(1): 1–17.

[25] Otsuka N, Liu M-H, Shiota S, Ogawa W, Kuroda T, Hatano T, Tsuchiya T. Anti-methicillin resistant *Staphylococcus aureus* (mrsa) compounds isolated from *Laurus nobilis*. *Biol Pharm Bull*. 2008; 31(9): 1794–1797.

[26] Biglar M, Soltani K, Nabati F, Bazl R, Mojab F, Amanlou M. A preliminary investigation of the jack-bean urease inhibition by randomly selected traditionally used herbal medicine. *Iran J Pharm Res*. 2012; 11(3): 831–837.

[27] Biglar M, Sufi H, Bagherzadeh K, Amanlou M, Mojab F. Screening of 20 commonly used iranian traditional medicinal plants against urease. *Iran J Pharm Res*. 2014; 13(S): 195–198.

[28] Golbabaei S, Bazl R, Golestanian S, Nabati F, Omrany ZB, Yousefi B, Hajiaghaee R, Rezazadeh S, Amanlou M. Urease inhibitory activities of β-boswellic acid derivatives. *DARU J Pharm Sci*. 2013; 21(1): 1–6.

[29] O'Shannessy DJ, Brigham-Burke M, Peck K. Immobilization chemistries suitable for use in the BIAcore surface plasmon resonance detector. *Anal Biochem*. 1992; 205(1): 132–136.

[30] Puiu M, Istrate O, Rotariu L, Bala C. Kinetic approach of aflatoxin B1-acetylcholinesterase interaction: a tool for developing surface plasmon resonance biosensors. *Anal Biochem*. 2012; 421(2): 587–594.

[31] Morris GM, Huey R, Lindstrom W, Sanner MF, Belew RK, Goodsell DS, Olson AJ. Autodock4 and autodocktools4: automated docking with selective receptor flexibility. *J Comput Chem*. 2009; 30(16): 2785–2791.

[32] Ajayi OB, Akomolafe SF, Akinyemi FT. Food value of two varieties of ginger (*Zingiber officinale*) commonly consumed in Nigeria. *ISRN Nutrition*. 2013; Article ID

359727.

[33] Jabbari S, Dabirmanesh B, Khajeh K. Specificity enhancement towards phenolic substrate by immobilization of laccase on surface plasmon resonance sensor chip. *J Mol Catal B: Enzym*. 2015; 121: 32–36.

[34] Savara A, Schmidt CM, Geiger FM, Weitz E. Adsorption entropies and enthalpies and their implications for adsorbate dynamics. *J Phys Chem C*. 2009; 113(7): 2806–2815.

[35] Wassaf D, Kuang G, Kopacz K, Wu QL, Nguyen Q, Toews M, Cosic J, Jacques J, Wiltshire S, Lambert J, Pazmany CC, Hogan S, Ladner RC, Nixon AE, Sexton DJ. High-throughput affinity ranking of antibodies using surface plasmon resonance microarrays. *Anal Biochem*. 2006; 351(2): 241–253.

[36] Strehlitz B, Gründig B, Kopinke H. Sensor for amperometric determination of ammonia and ammonia-forming enzyme reactions. *Anal Chim Acta*. 2000; 403(1): 11–23.

[37] Qin W, Zhang Z, Li B, Peng Y. Chemiluminescence flow system for the determination of ammonium ion. *Talanta*. 1999; 48(1): 225–229.

Abbreviations

SPR: plasmon resonance biosensor; AFM: atomic force microscopy; CMD: carboxymethyldextran; NHS: N-hydroxysuccinimide; EDC: N-ethyl-N′-(3-dimethylaminopropyl) carbodiimide.